

Knock Out Slow Extraction Using Betatron Sidebands at High Harmonics

Philipp Niedermayer * and Rahul Singh 

GSF Helmholtzzentrum für Schwerionenforschung, Darmstadt, Germany

Eike Feldmeier , Christian Schömers , and Marcel Hun
Heidelberg Ion-Beam Therapy Center (HIT), Heidelberg, Germany

Radio frequency knock out resonant slow extraction is a standard method for extracting stored particle beams from synchrotrons by transverse excitation. Excitation signals comprising many betatron sidebands have shown to reduce intensity fluctuations of the extracted beam spill and are used at several facilities. In this contribution, the effect of individual sidebands at different harmonics on the spill quality is systematically studied. Particle tracking simulations show a clear correlation between the chosen excitation frequency, the spectrum of particle motion shortly before their extraction, and the spill quality. Experiments confirm these observations while highlighting the reduction of pile-up when using higher excitation frequencies. These insights have implications for an optimal design of excitation waveforms and hardware for Knock Out extraction systems.

Keywords: Slow extraction, Beam excitation, Spill quality, Pile-up

I. INTRODUCTION

Radio Frequency Knock Out (RF-KO) resonant slow extraction is used to extract stored particle beams from synchrotron rings [1, 2]. It utilizes a working point near a sextupole-driven third-integer resonance to create a transverse, betatron amplitude dependent instability [3]. The beam is driven into the instability in a controlled manner by increasing the particle amplitude through transverse radio frequency (RF) excitation. The excitation system consists of a signal generator, amplifiers and a stripline kicker [4], inside which the electromagnetic RF field deflects traversing particles on each turn. Over several hundred turns, these transverse kicks lead to a net change of the particle amplitudes, bringing them closer to the separatrix. On crossing the separatrix, particle becomes unbound and septa are used to deflect these particles into an extraction beam line. A *spill* of extracted particles is then delivered to experiments or used for medical therapy.

A particular challenge in resonant slow extraction are fluctuations of the spill intensity on various timescales. As large fluctuations reduce the efficiency of beam usage, this is referred to as a low spill quality [5, 6]. Numerous efforts have been made in the past seven decades to address this particular challenge [7–16]. More recently, the simultaneous excitation of multiple betatron sidebands at different revolution harmonics has been investigated. A study at the Wakasa Wan Energy Research Center (WERC) used simulations and experiments to show, that excitation signals covering the first N sidebands progressively improve the spill quality as more sidebands are added [17]. These excitation signals consisted of a series of noise bands around each betatron sideband and are referred to as *many-band* signals in the following. In a

study at the Heidelberg Ion Beam Therapy Center (HIT), excitation signals comprising three frequencies at two different sidebands were found to significantly improve the spill quality compared to the previously used single-band signal covering the 1st betatron sideband only [18]. This excitation scheme used narrowband random binary phase-shift keying (RBPSK) signals with frequencies near $1/3$ and $4/3$ of the revolution frequency.

In this contribution, the excitation of individual sidebands is systematically investigated using simulations and experiments. The effect of each sideband on the spill quality is characterized and compared to the combined excitation of two or more sidebands at low and high harmonics. Finally, the implications of these findings for the design of RF-KO excitation systems are discussed.

A. Betatron sidebands

The betatron tune $Q_x = Q_{x,\text{ref}} + \xi_x \delta$ describes the number of betatron oscillations a particle performs each turn and depends on the particle's momentum deviation $\delta = \Delta p/p_{\text{ref}}$ via the chromaticity ξ . In the following, the lowercase $q_x \leq 0.5$ defined as distance to the nearest integer is used. At a fixed location in the synchrotron, the betatron motion modulates the transverse particle position

$$x(s, t) = \sqrt{\epsilon_x \beta_x(s)} \cos(2\pi Q_x t + \mu_x(s) + \Phi_x)$$

where $t \in \mathbb{N}_0$ is the integer turn number and $s < C$ the location along the orbit with circumference C . The amplitude is given by ϵ_x and the beta-function $\beta_x(s)$ and the phase is given by Φ_x , Q_x and the phase advance function $\mu_x(s)$ with $\mu_x(C) = Q_x$. Due to this turn-by-turn modulation, spectra of the transverse beam motion are dominated by the well known betatron sidebands at

$$f_{\pm} = (h \pm k q_x) f_{\text{rev}} \quad (1)$$

* p.niedermayer@gsi.de

where $h \in \mathbb{N}_0$ is the nearby harmonic of the revolution frequency f_{rev} and $k \in \mathbb{N}$ accounts for the appearance of second and higher order betatron sidebands. These higher order sidebands are the consequence of an additional frequency modulation caused by the nonlinear motion in the vicinity of the sextupole-driven third-integer resonance [19]. In the following, the discussion is limited to the dominant first-order sidebands for which $k = 1$.

B. Spill quality

To assess the quality of a spill, the intensity of the extracted beam is recorded as the particle count N per time interval Δt_{count} . Fluctuations of the intensity are then evaluated over a time period Δt_{eval} using the standard deviation $\sigma_N = \sqrt{\langle (N - \langle N \rangle)^2 \rangle}$ and mean $\mu_N = \langle N \rangle$. From these, the coefficient of variation c_v and the equivalent spill duty factor F are calculated as [6]

$$c_v = \frac{\sigma_N}{\mu_N} = \sqrt{\frac{\langle N^2 \rangle}{\langle N \rangle^2} - 1} \quad F = \frac{1}{1 + c_v^2} = \frac{\langle N \rangle^2}{\langle N^2 \rangle}$$

where a smaller c_v and larger F corresponds to a better spill quality. For the ideal case of a Poisson process with $\sigma_N = \sqrt{\mu_N}$, the coefficient of variation is $c_v = \langle N \rangle^{-1/2}$. In the following, $\Delta t_{\text{eval}} = 1000 \Delta t_{\text{count}} = 100 \text{ ms}$ is used.

In addition, the delay between the extraction of consecutive particles is of interest to quantify the amount of pile-up. Considering a detector system which requires a separation time of at least $\Delta t_{\text{pile-up}}$ to distinguish and resolve single events, pile-up is defined by the fraction of inter-particle-delays smaller than $\Delta t_{\text{pile-up}}$. In the following, $\Delta t_{\text{pile-up}} = 5 \text{ ns}$ is used in simulations and 20 ns for evaluation of experimental data.

C. Simulation framework

Particle tracking simulations of the RF-KO extraction process are performed with Xsuite [20], using the lattice of the HIT synchrotron [21] with the parameters listed in table I. The individual tune of particles deviates from the working point $Q_{x,\text{ref}}$ due to chromatic and amplitude detuning [22], and is limited by the nearby third-integer resonance $Q_{\text{res}} = 5/3$ where particles are extracted. To cover this range, an excitation signal with a rectangular spectral density with full bandwidth $\Delta Q_{\text{ex}} = 0.02$ is used. A band-filtered noise signal is chosen because of its homogeneous spectral density. This avoids the large influence of the central frequency on the spill quality as observed for narrowband excitation signals [23], which would dominate and hinder the investigation of the behaviour at different sidebands. The amplitude of the excitation signal is controlled with a feedback system to achieve a constant spill rate of $\dot{N} = 5 \times 10^5$ particles/s as given by the number of 10^6 ions and the extraction time

TABLE I. Beam, optics and excitation parameters

Ion	Carbon $^{12}\text{C}^{6+}$	
Energy	$E_{\text{kin}}/m = 251 \text{ MeV}/u$	
Momentum	$p_{\text{ref}} = 8.74 \text{ GeV}/c$	
Rigidity	$B\rho = 4.86 \text{ T m}$	$E\rho = 897 \text{ MV}$
Lorentz factor	$\gamma = 1.27$	$\beta = 0.616$
Rev. frequency	$f_{\text{rev}} = 2.842719 \text{ MHz}$	
Norm. emittance	$\epsilon_{\text{xn}} = 1.5 \text{ mm mrad}$	
Momentum spread	$\delta_{1\sigma} = 1 \times 10^{-3}$	
Betatron tune	$Q_{x,\text{ref}} = 1.6790$	$Q_{y,\text{ref}} = 1.7550$
Chromaticity	$\xi_x = -1.59$	$\xi_y = -1.99$
Sextupole	$S = 27.9 \text{ m}^{-1/2}$	$\mu_S = -2.9^\circ$
Transition	$\gamma_{\text{tr}} = 1.82$	$\alpha_p = 0.30$
Slip factor	$\eta = \gamma^{-2} - \gamma_{\text{tr}}^{-2} = 0.32$	
Excitation signal	Band-filtered noise	
Central frequency	$Q_{\text{ex}} = f_{\text{ex}}/f_{\text{rev}} = h \pm 0.327$	
Bandwidth	$\Delta Q_{\text{ex}} = \Delta f_{\text{ex}}/f_{\text{rev}} = 0.02$	

of 2 s used in the simulations. To model disturbances from the electrical grid, ripples on the quadrupole magnets comprising the dominant harmonics of the mains frequency at 100, 250 and 300 Hz as well as noise up to 10 kHz with a relative magnitude of 10^{-5} are added [24].

II. SPILL QUALITY FOR SINGLE-BAND EXCITATION

The RF-KO extraction process is simulated as described above and the resulting spills are evaluated. Figure 1 shows the spill quality obtained as a function of the respectively excited sideband. A significant improvement is observed when exciting sidebands of higher revolution harmonics. This trend is in agreement with the findings obtained for many-band excitation at WERC [17], however, the improvement is already observed for single-band excitation at the higher frequencies. The excitation power required at these frequencies is only marginally larger compared to lower frequencies (about 3 dB, see figure 1, bottom).

At the commonly used lower excitation frequencies near the first few harmonics, a systematic difference between the excitation of upper and lower sidebands is observed. In the case presented here, the spill quality is improved by exciting a sideband at $h + q_x$ instead of a nearby sideband at $h - q_x$. With about a factor two, this effect is largest for the two sidebands around $h = 2$. However, as shown in section II B, the role of the sidebands, the magnitude and location of the maximum value of c_v and the limit of c_v towards high excitation frequencies are specific to the properties of the beam and lattice.

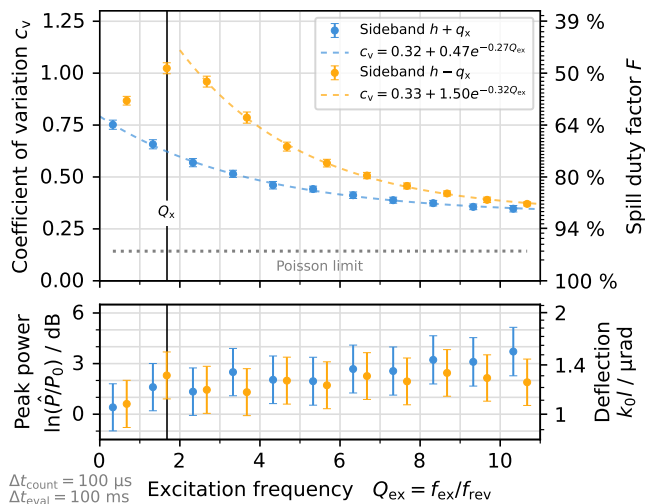


FIG. 1. Spill quality (top) and excitation power (bottom) as function of excitation frequency for the case of exciting a single betatron sideband. Simulation result.

A. Imprint of excitation frequency onto spill

In resonant slow extraction, the spill quality is dominated by intensity fluctuations of typically up to a few 10 kHz. In addition, for RF-KO, the excitation frequency and its harmonics are imprinted onto the spill to some extent. This is an intrinsic property of the RF-KO method and the consequence of coherent beam oscillations at these frequencies induced by the excitation. The resulting spill structures of typically a few MHz are not relevant for facilities like HIT dedicated to hadron cancer therapy applications. However, for high intensity particle physics experiments such as those at GSI and the Facility for Antiproton and Ion Research (FAIR), the imprint of these frequencies is undesired as it can facilitate the extraction of particles in short succession (pile-up). This is especially problematic when the dominant low frequency fluctuations cause a momentary increase of the extraction rate, temporarily increasing the probability for pile-up.

The simulations show that the imprint of the excitation frequency can be mitigated by exciting an appropriate sideband at a higher revolution harmonics. Figure 2 shows how both – fluctuations at low frequencies and the imprint at the excitation frequency – are suppressed in the same manner as the spill quality improves. For high intensity particle physics experiments, this means that the probability for pile-up is reduced in two ways: First, the suppression of low frequency fluctuations avoids the temporary increase of the extraction rate that facilitates pile-up. Second, the mitigation of the high frequency imprint additionally reduces the probability for particles being extracted in short succession. As a result, pile-up is reduced as a function of the excitation frequency in analogy to the spill quality as shown in figure 3.

B. Influence of beam and optics parameters

To further study the role of upper and lower sidebands, it is useful to generalize the description of the excitation signal to negative frequencies. For a real-valued excitation signal, frequencies below zero are the mirror image of the positive spectrum and result in the same physical signal being applied to the beam. By changing the sign of the excitation frequency for the sidebands at $h + q_x$, the treatment of upper and lower sidebands can be unified. With the excitation frequency defined as $Q_{\text{ex}} \approx h_0 + q_x$ where $h_0 \in \mathbb{Z}$ can be negative, the improvement of the spill quality becomes symmetric with respect to the maximum, saturating towards large $|h_0|$ and following a double exponential curve. However, this functional dependency is subjected to a number of beam and machine parameters, which is discussed in the following.

The relative **momentum spread** $\delta_{1\sigma} = \Delta p_{1\sigma}/p_{\text{ref}}$ of the beam determines how rapidly the spill quality improves as sidebands further away from the maximum are excited (figure 4, top). In the limit of a vanishing momentum spread, no difference between the excitation of different sidebands is observed. A larger momentum spread is beneficial and reduces spill fluctuations not only at lower excitation frequencies but especially when exciting sidebands at higher frequencies. Also, the difference in spill quality between upper and lower sidebands is magnified as a function of the momentum spread. The required excitation power is independent of the momentum spread, as long as the excitation covers the momentum dependent tune spread of the beam (here $\delta_{1\sigma} \lesssim 2 \times 10^{-3}$).

The **chromaticity** $\xi_x = \Delta Q_x/\delta$ of the lattice influences the location of the maximum value of c_v (figure 4, middle). An inversion of the sign of the chromaticity causes the roles of upper and lower sidebands to interchange, while for zero chromaticity they behave identically and the spill quality improves purely as a function of excitation frequency or harmonic. In analogy to the momentum spread, a large chromatic tune spread exceeding the excitation band leads to an increased power requirement for $|\xi| \gtrsim 2$.

The **slip factor** $\eta = \gamma^{-2} - \gamma_{\text{tr}}^{-2}$ depends both on the beam energy $E = \gamma E_0$ and the lattice's gamma transition γ_{tr} . It influences the sharpness of the spill quality improvement by acting as a scaling factor on Q_{ex} (figure 4, bottom). For a larger absolute value of the slip factor (smaller beam energy) the spill quality improvement has a stronger correlation with increasing excitation frequency. For small excitation frequencies at the first sideband, however, the spill quality is largely independent of the slip factor. While the excitation power naturally scales with the beam energy, its dependence on the excitation frequency is independent of the slip factor.

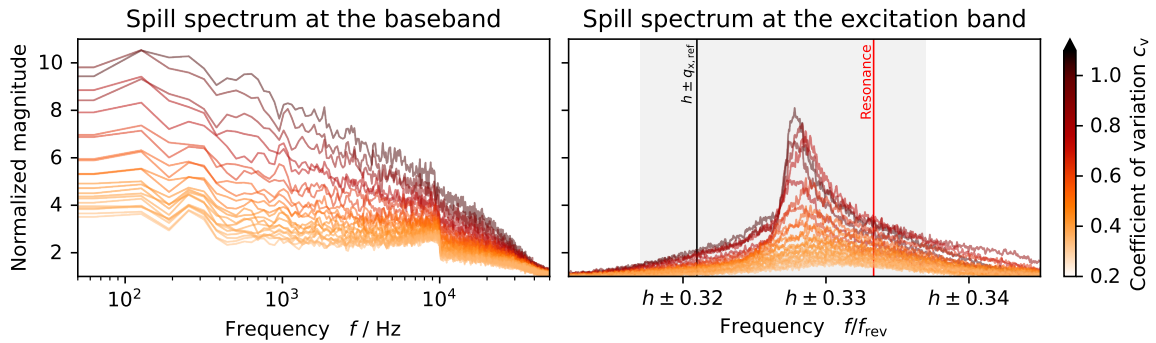


FIG. 2. Spill spectra for the simulation results from figure 1 at the baseband (left) and at the respective excitation band (right). The color correlates with the coefficient of variation, thus lighter shades correspond to higher excitation frequencies according to figure 1. Vertical lines mark the location of tune and resonance in the respective band, and the gray shading marks the extent of the excitation band.

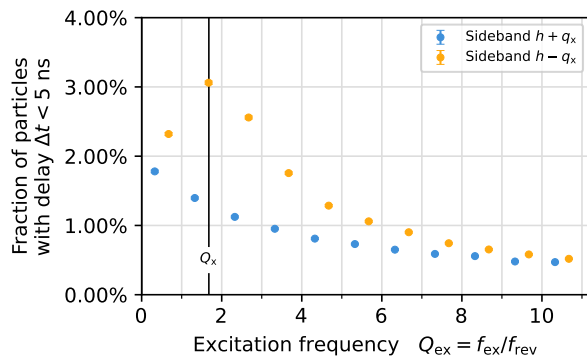


FIG. 3. Amount of pile-up as function of excitation frequency for the case of exciting a single betatron sideband. Pile-up is expressed in terms of the fraction of particles which are separated by less than $\Delta t_{\text{pile-up}} = 5$ ns. Simulation result.

III. SCHOTTKY SPECTRA OF STRONG NONLINEAR BEAM MOTION

The functional dependence of the spill quality on the excitation frequency as well as the momentum spread, tune, chromaticity and slip factor discussed in section II B suggests, that it is related to the spectral properties of the respective sidebands as observed in Schottky spectra of a corresponding non-excited beam. For the case of linear particle motion, transverse Schottky spectra are well understood and the width of the sidebands at $f_{\pm} = (h \pm q_x)f_{\text{rev}}$ is given by [25]

$$\Delta f_{\pm} = |(h \pm q_x)\eta \pm \xi_x| \frac{\Delta p}{p_{\text{ref}}} f_{\text{rev}} \quad (2)$$

with the parameters from table I and the plus and minus signs for the upper and lower sidebands respectively. Since this functional dependence does not account for the nonlinear dynamics near the third-integer resonance used for RF-KO extraction, it does not describe the observed spill quality improvement.

A. Nonlinear and hollow beam spectra

To adapt the linear description of Schottky spectra to the nonlinear case, an additional detuning term ν_{det} is added to equation (2):

$$\frac{\Delta f_{\pm}}{f_{\text{rev}}} = \nu_{\text{det}} + |(h \pm q_x)\eta \pm \xi_x| \frac{\Delta p}{p_{\text{ref}}} \quad (3)$$

The detuning term ν_{det} accounts for the nonlinear amplitude detuning towards the third-integer resonance [19, 26], and depends on the distance of the working point to the resonance and the beam distribution inside the separatrix (given by the beam emittance and separatrix size). In figure 5 (bottom), the sideband widths in the simulated Schottky spectrum of a full beam are shown by gray cross markers. The dotted gray line shows that equation (3) is suited to describe the Schottky widths using the parameters from table I and $\nu_{\text{det}} = 0.00113(4)$ as determined by a fit. While both are in good agreement, the dependency is still not suited to describe the spill quality improvement of figure 1. This is because the Schottky spectrum of the stored beam is dominated by the majority of particles at low betatron amplitudes near the beam core, while the extraction process is governed solely by particles near the separatrix. Therefore, a hollow beam distribution comprising only particles near the separatrix which are about to be extracted is considered instead. This beam distribution is depicted in figure 6. From the particle tracking simulations, it is possible to obtain Schottky spectra of such a non-excited hollow beam. This spectrum is shown in figure 5 (top) and represents only the strongly nonlinear motion near the separatrix. As can be seen in figure 5 bottom, in this case, the width of the respective sideband shows the same behaviour as the spill quality improvement obtained by exciting the respective sideband (compare figures 1 and 5). The sideband at $2 - q_x$ has the smallest width, resulting in the worst spill quality, while the spill quality improves along with the increasing sideband width for sidebands at $h + q_x$ and towards higher frequencies.

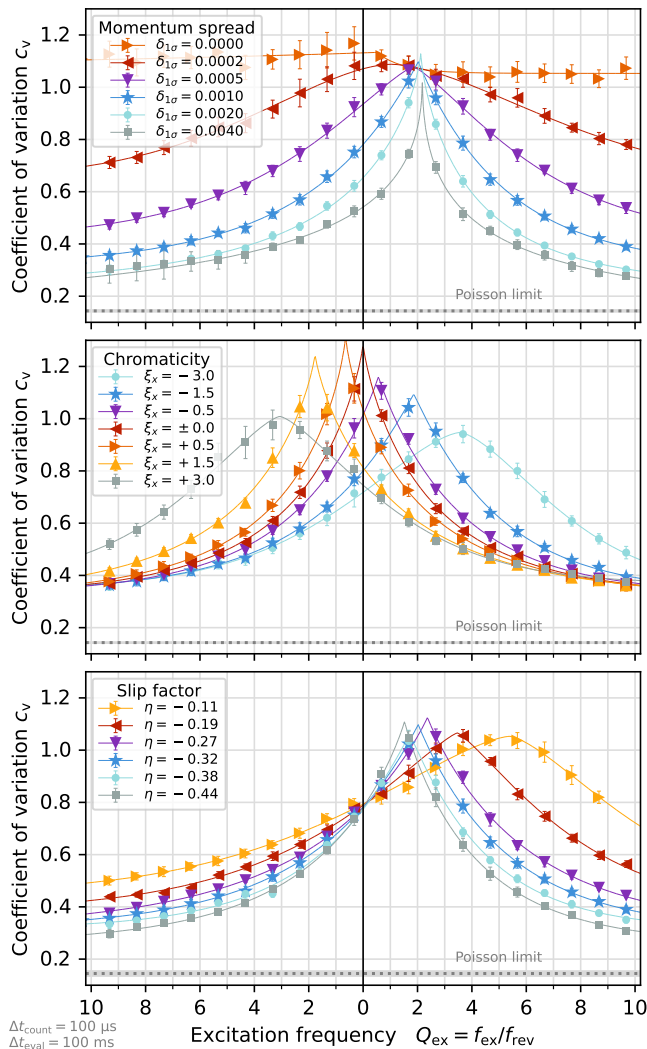


FIG. 4. Spill quality as function of excited sideband and momentum spread (top), chromaticity (middle) and slip factor (bottom). In each plot, the case of $\delta_{1\sigma} = 0.001$, $\xi = -1.5$ and $\eta = -0.32$ (blue stars) corresponds to figure 1. Sidebands at $h+q_x$ are shown as mirrored to the left half, while sidebands at $h-q_x$ are shown on the right half. Solid lines are added purely to guide the eye. In the simulation, the slip factors correspond to different beam energies between $E_{\text{kin}} = 150 \text{ MeV/u}$ for $\eta = -0.44$ and 500 MeV/u for $\eta = -0.12$.

B. Correlation with spill quality

The correlation between the spill quality and the width of the sidebands in the spectra of a hollow beam also remains valid if the parameters discussed in section II B are changed. Figure 7 shows this correlation between the sideband width obtained from hollow beam simulations without excitation and the spill quality of the corresponding RF-KO extraction simulations for various optics settings. This correlation can be understood as follows: A larger sideband width in the hollow beam spectrum means, that the frequency spread of the nonlinear beta-

tron motion particles perform near the third-integer resonance separatrix is larger. A broadband excitation with frequencies ranging from the working point to the resonance can then couple more homogeneously to the beam as particles transit from the core to the separatrix. The result is a “resistive” excitation process with a larger net energy transfer to the beam. On the other hand, if the resonant frequency spread of the beam is small compared to the excitation bandwidth, the process is “reactive”, resulting in an oscillatory motion and a stronger imprint of the non-resonant part of the excitation spectrum is observed on the spill.

Further, the extraction process can be understood as a demodulation of the excitation spectra by the beam spectra, causing the “overhanging” excitation frequencies to be transformed onto the spill structure in baseband. The spill spectrum is therefore dominated by the demodulated excitation signal spectrum in the baseband at low frequencies (compare figure 2, left), after it has been filtered through the extraction process with its characteristic transit time spread. An obvious way to reduce this imprint is by reducing the excitation bandwidth [18], or using a sinusoidal signal with zero bandwidth [23]. However, such a single frequency excitation cannot efficiently drive the RF-KO extraction, because it cannot account for the intrinsic amplitude detuning from the beam core to the separatrix. As such, these methods rely on a higher excitation power, or a combination of multiple narrower and broader bands, and require that the excitation signal parameters are tuned to the beam spectra using dynamic signal generators with an optimization algorithm [27]. Generally, to maximize the net energy transfer throughout the transition of particles from the core to the separatrix, a broadband excitation signal has to be used. In this case, exciting the beam at a sideband where the spectrum of particle motion is broader has the same effect of mitigating the imprint of the excitation, since the excitation matches the spectrum of particles near the separatrix better. This reduces unmatched frequencies to be imprinted onto the spill in baseband and at the excitation frequency harmonics, which results in a better spill quality as discussed earlier. For this process, the width as obtained from a hollow beam distribution is determining, since only the spectrum of particles near the separatrix is relevant for the extraction process.

IV. COMPARISON TO DUAL AND MANY-BAND EXCITATION

Figure 8 shows the spill quality obtained with single-band excitation as discussed above (circle markers) in comparison to several dual- (rhomb markers) and many-band excitation signals (triangle markers). Here, a dual-band signal is the sum of two single-band signals located at different sidebands and a many-band signal is the sum of all single-band signals at upper, lower or both sidebands respectively, from the lowest sideband up to the

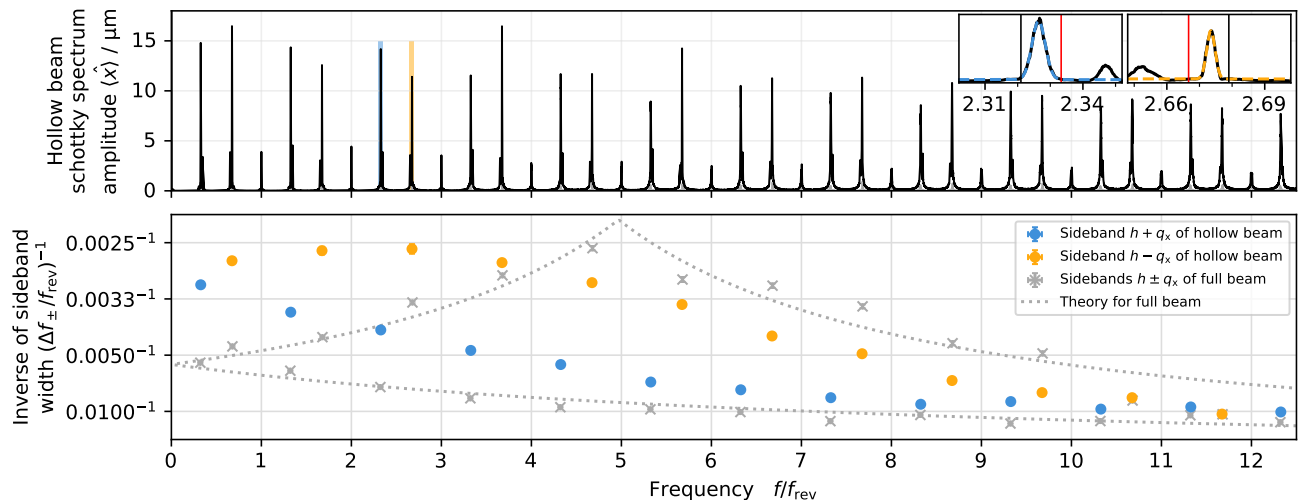


FIG. 5. Simulated transverse Schottky spectrum of a hollow beam with betatron sidebands (top) and inverse of their 1-sigma widths (bottom, blue/orange) as obtained from Gaussian fits. The insets show zooms for the two highlighted sidebands, including the respective fit result. The small additional peak visible therein is the second order sideband $k = 2$ (compare equation (1)). The gray marks in the bottom plot are the sideband widths for the case of a full (not hollow) beam and the dotted gray line is the corresponding theoretical prediction according to equation (3) for a detuning term of $\nu_{\text{det}} = 0.00113(4)$.

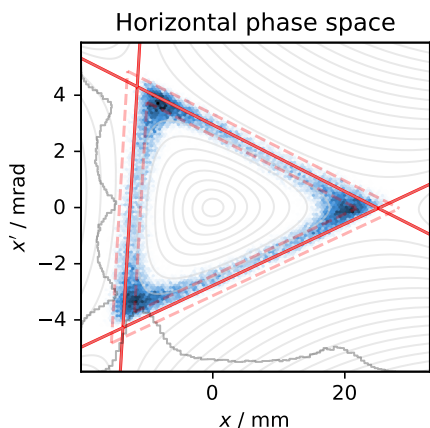


FIG. 6. Horizontal phase space distribution of a hollow beam (corrected for closed orbit and dispersion). The beam occupies the outer 10% in terms of the Hamiltonian (equipotentials marked by thin gray lines). The red lines mark the separatrix of the third-integer resonance for a momentum offset of $\delta = 0$ (solid) and $\delta = \pm 10^{-3}$ (dashed) respectively.

indicated frequency.

For the many-band cases, the spill quality improves with the number of bands, as the combination of multiple frequencies leads to a smoothing of the spill structure. This is in agreement with the previous findings at HIT [18] and WERC [17]. In a simplified picture, the extracted spill can be understood as the average over many spills obtained from simultaneous extractions, each from a distinct excitation sideband. Since the many-band excitation always contains contributions from the lower harmonics which have a lower spill quality, the correlation of

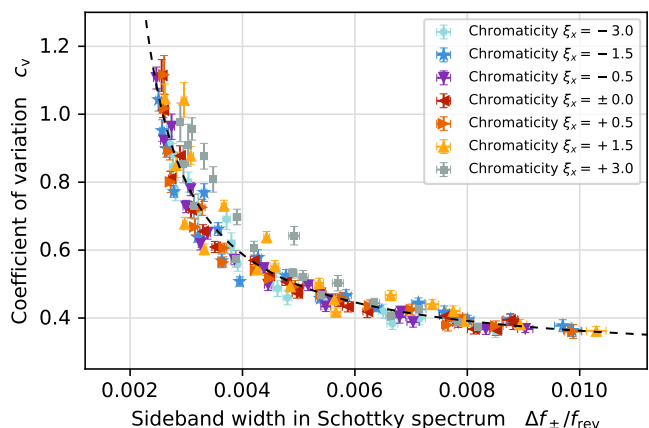


FIG. 7. Correlation between the width of a sideband in the Schottky spectrum of a hollow beam (compare figure 5) and the spill quality resulting from its excitation, obtained from simulations with various optics settings (compare figure 4, middle). The excitation bandwidth is with $\Delta Q_{\text{ex}} = 0.02$ always larger than the sideband width. The fit function (dashed line) is $c_v = 0.27(2) + 0.8(1)/[10^3 \Delta f_{\pm}/f_{\text{rev}} - 1.5(1)]$ where the numbers in brackets denote the uncertainty on the least significant digit.

the spill quality with the excitation frequency is weaker compared to a single-band excitation. In addition, the imprint of these low frequencies onto the spill increases pile-up as discussed above. As a result, single- or dual-band excitations at (only) the high harmonics result in a better spill quality than any many-band case containing lower harmonics. Thereby, dual-band excitation performs better than single-band excitation, following the same argument that multiple frequencies lead to a spill

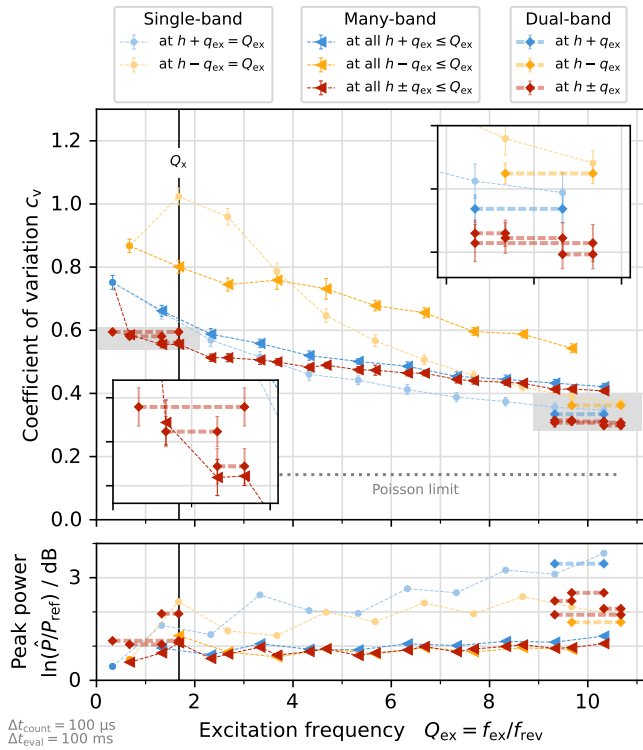


FIG. 8. Spill quality (top) and excitation power (bottom) as function of the excited sidebands. The plot shows: The single-band cases from figure 1 for reference (circle markers); Many-band cases with simultaneous excitation of the first n upper, first n lower, or all first n sidebands up to the indicated frequency (triangle markers); Dual-band cases with simultaneous excitation of two upper, two lower, or one upper and one lower sideband at the two indicated frequencies (pairs of rhomb markers connected by wide dashed line). The shaded regions are enlarged in the inset plots. The reference power $P \propto (k_0 l)^2$ corresponds to a deflection of $k_0 l_{\text{ref}} = 1 \mu\text{rad}$. Simulation result.

smoothing. This combination of two sidebands is akin to frequency multiplexing of two RF-KO extraction processes. Similarly, the well known Dual FM method [10] can be thought of as time multiplexing of two RF-KO processes.

In all of the cases depicted in figure 8, the combination of upper and lower sidebands results in an additional improvement of the spill quality compared to exciting either type alone. This can be attributed to the detuning from the zero-amplitude tune $Q_x = h \pm q_x$ to the resonance $Q_{\text{res}} = h \pm 1/3$, which corresponds to a frequency change that is in opposite direction for upper and lower sidebands respectively. As a consequence, the excitation signal can couple to particles with different detuning simultaneously through the two sidebands, for example to particles near the core via the upper sideband and particles near the separatrix via the lower sideband, which leads to a more homogeneous excitation process and a smoother spill as described above. For the case of using two upper (or two lower) sidebands, however, the detun-

ing is unipolar and there is no difference in the excitation of particles via two sidebands.

Single- or dual-band excitations at high harmonics are not only beneficial in terms of the spill quality. They can also simplify the design of excitation systems compared to the many-band case spanning many harmonics, since a much smaller system bandwidth is required. For example, exciting the upper and lower sideband of the 20th harmonic would require a system bandwidth of only 10% of the tunable central frequency. The reduced demand in terms of frequency characteristics could allow for a higher impedance power coupling mechanisms with less power losses [17].

V. COMPARISON TO MEASURED SPILLS

In a dedicated experiment at the Heidelberg Ion Beam Therapy Center (HIT), the spill quality and amount of pile-up was measured as a function of the excitation frequency.

A. Measurement setup

The experiment was carried out at one of HIT's therapy beam lines. A $^{12}\text{C}^{6+}$ beam with $E_{\text{kin}} = 251 \text{ MeV/u}$ ($f_{\text{rev}} = 2.8438 \text{ MHz}$) was utilized, the horizontal betatron tune was set to $Q_{x,\text{ref}} = 1.6802$ and the nominal chromaticity was $\xi_x = -0.655$. While for treatment purposes the RF-KO extraction is performed with the beam bunched by the accelerating RF cavity, bunching was turned off for the following measurements to simplify the beam dynamics interpretation and allow for a closer comparison to the simulations. The initial beam momentum spread was measured to be $\delta_{1\sigma} \approx 7 \times 10^{-5}$ using a longitudinal Schottky monitor.

HIT's excitation system consists of a signal generator based on direct digital synthesis (DDS), a 500 W power amplifier with a bandwidth of 20 MHz and a 50 Ω terminated stripline exciter. The exciter's electrode plates have a physical length of 0.75 m and an electrical length of 1.1 m each (measured between the vacuum feed-throughs). They are connected in series with cables and a transformer in between, which is designed to invert the signal polarity at frequencies below 2 MHz in order to create the transverse deflecting RF field between both electrodes. Given this serial connection scheme, an additional frequency dependent phase shift is introduced by the total length of the signal path between the plates. At about $17 \text{ MHz} \approx 6 f_{\text{rev}}$ the additional shift amounts to 180° , which including the transformer leads to a total phase shift of about 360° between the plates, effectively causing the transverse RF field to vanish. The transverse field of the exciter has another maximum at about $34 \text{ MHz} \approx 12 f_{\text{rev}}$, where the total phase shift amounts to 540° .

For the measurement, RF-KO extraction was performed for two scenarios: First, with the RBPSK excitation and spill intensity feedback system as used for treatment, and second, with a band-filtered noise excitation of manually adjusted amplitude. In both cases, a central frequency and bandwidth according to [table I](#) was used. The spills were recorded with an Ionisation Chamber (IC) at 50 μs resolution for analysis of the spill quality. In addition, a BC400 plastic scintillator connected to a photomultiplier was installed downstream of the IC to record the last 18 ms of the spill with an oscilloscope at 0.32 ns resolution. The scintillator pulses were analysed with individual particle pulse detection using the standard peak detection algorithm `signal.find_peaks` of the `scipy` library [28]. The resulting timestamps are used for the pile-up analysis.

B. Measured spill quality and pile-up

The spill quality measured at an extraction rate of 2×10^7 with the nominal machine settings as stated above is shown in [figure 9](#) as a function of the central frequency of the single-band RBPSK excitation signal. The spill quality gradually improves for higher sidebands, and there is a small yet systematic difference between excitation at lower and upper betatron sidebands. There is a fair agreement of the measured spill quality with the corresponding simulation in [figure 4](#) (top). The measured effect is small compared to the simulation due to the low beam momentum spread during the experiment. It was not possible to extract the desired intensity at the band corresponding to $Q_{\text{ex}} = 6.327$ with HIT's excitation system due to its frequency characteristic as explained above.

Under the same machine settings but at a lower extraction rate of 4 MHz, individual particles were recorded with the scintillator and analysed for pile-up. The cumulative distribution of the measured time between consec-

utive particles is shown in [figure 10](#) (left). In the figures, also a selected region of 2 μs of the raw signal with piled-up pulses is highlighted. It can be seen that the predominant periodicity of particles is defined by the excitation frequency, resulting in clustering at a lower excitation frequency. With the scintillator pulse full width at half maximum (FWHM) being about 25 ns, consecutive particles arriving within this period would pile-up. By evaluating the fraction of particles arriving within less than $\Delta t_{\text{pile-up}} = 20 \text{ ns}$, the amount of pile-up is shown as a function of excitation frequency in [figure 10](#) (right). Inline with the expectations, pile-up reduces as the excitation frequency increases with respect to the average particle rate. This also suggests that the excitation frequency can be utilized as a free parameter to match the desired rate of a detector system.

While repeating the measurements at a higher absolute value of the chromaticity of $\xi = -2.656$, it was possible to extract particles also at larger frequencies, including the region above the 6th harmonic where the frequency response of the excitation system is damped as described above. In this case, the second order sidebands become visible in the spill spectra ([figure 11](#)). These second order sidebands can also be seen in the Schottky simulations ([figure 5](#), insets). The spill quality and the particle arrival plots discussed earlier are shown again for this chromaticity value also for larger excitation frequencies in [figures 12](#) and [13](#). The conclusions drawn for nominal chromaticity concerning spill quality and pile-up also hold for this case.

Finally, for the nominal chromaticity setting, [figure 14](#) shows a comparison of the spill quality of single- and dual-band excitation signals. In agreement with the simulations, a significant improvement is observed by combining one upper and one lower sideband as discussed above. This holds true for two low as well as two high excitation frequency bands.

VI. CONCLUSION

Detailed simulations of coasting beam Radio Frequency Knock Out (RF-KO) extraction by exciting sidebands at various harmonics individually as well as in different combinations were presented for the HIT synchrotron. The simulations suggest a strong correlation of the spill quality with the spread of betatron oscillation frequencies of particles near the separatrix which are about to be extracted. Thereby, the overlap of the excitation band with the intrinsic sideband width for these particles is decisive. The latter strongly depends on the beam and ion optical settings, thus determining the spill quality. The dependence was investigated for the chromaticity, momentum spread and slip factor. Beam experiments at HIT were performed to verify the simulation outcomes. The observed trend of the spill quality improvement is small, which – given the low momentum spread under the experimental conditions – is in line

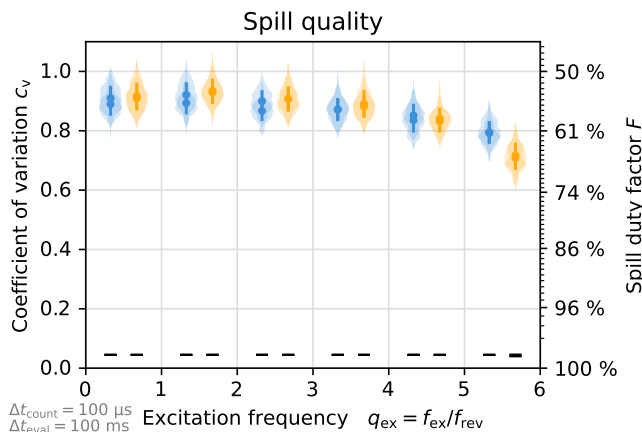


FIG. 9. Measured spill quality for single-band RBPSK excitation at sidebands of different harmonics.

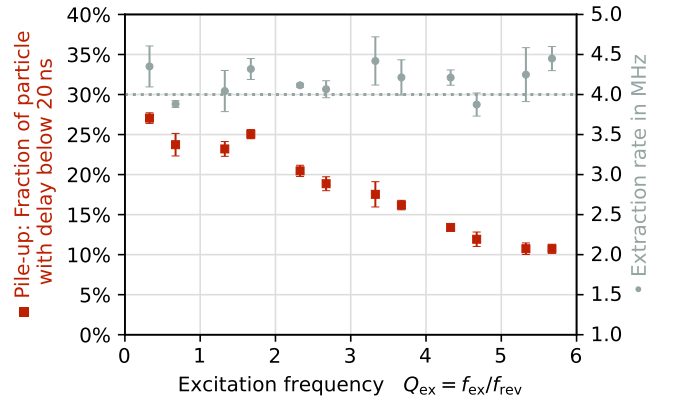
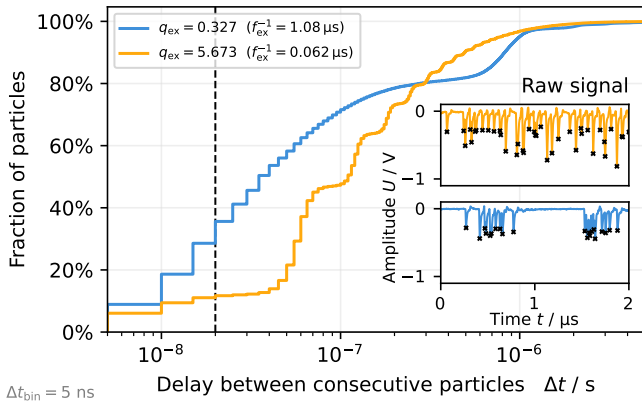


FIG. 10. Left: Cumulative distribution of particle arrival times for two excitation frequencies. The insets show the raw signal with pulses marked. Right: Fraction of particles arriving within 20 ns of each other (pile-up) as a function of the excitation frequency as well as corresponding extraction rate.

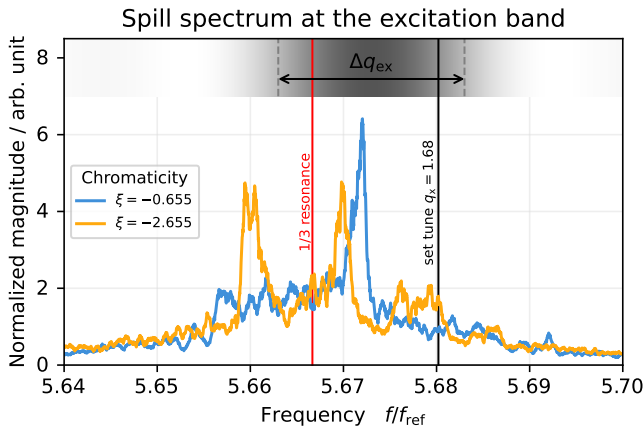


FIG. 11. Spill spectrum as recorded for the case of nominal and increased chromaticity. At the top, the spectral density of the RBPSK excitation is indicated by the color shading, and the -3 dB bandwidth is marked.

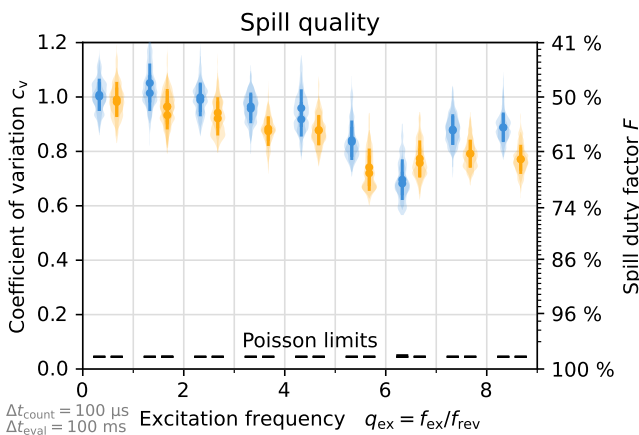


FIG. 12. Same as figure 9 but for the increased chromaticity of $\xi = -2.655$.

with the simulations. Generally, the experiment shows an improvement of the spill quality as well as a reduction of pile-up when exciting sidebands at higher harmonics. The mitigation of pile-up is especially relevant for high rate physics experiments, for which choosing higher excitation frequencies is preferable. Although a single sideband is already sufficient, a combined excitation of two high frequency sidebands shows an additional improvement. This is because of spill fluctuations being “washed out” by multiple uncorrelated excitations. In the studied case, one upper and one lower sideband gives the best result.

The results suggest that excitation systems for RF-KO extraction should be designed with the possibility of applying higher harmonic excitation to the beam. This does not only include the generation and amplification of the RF signals, but also the geometry and driving schema of the exciter electrodes. To avoid a frequency dependent phase shift, each electrode should be powered individually using identical signal path lengths. For non-relativistic beams also the electrode length must be large compared to the wavelength, limiting the accessible frequencies to a typical order of 100 MHz. Exciting only a single or two sidebands at a higher harmonics can potentially simplify the design of RF amplifiers, since the required bandwidth is only a small fraction of the revolution frequency as opposed to currently used broadband amplifiers covering many harmonics of the revolution frequency (as in [14, 17]).

When high frequencies are not accessible due to limitations of existing systems, spill improvement techniques utilizing multiple of the lower sidebands can be used. This includes the excitation of two or three of the lower sidebands (compare figure 14 and [18]), the usage of improved beam excitation signals [23] or the excitation of second order betatron sidebands [19]. While these techniques reduce low frequency fluctuations of the spill intensity, thus improving spill quality and reducing pile-up, a reduction of the excitation frequency imprint has not

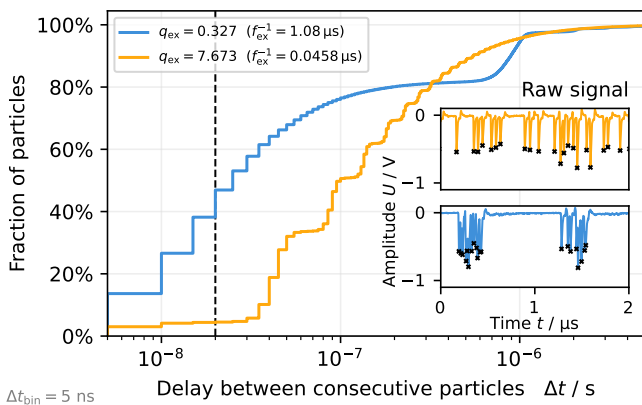


FIG. 13. Same as figure 10 but for the increased chromaticity of $\xi = -2.655$ and a larger range of excitation frequencies.

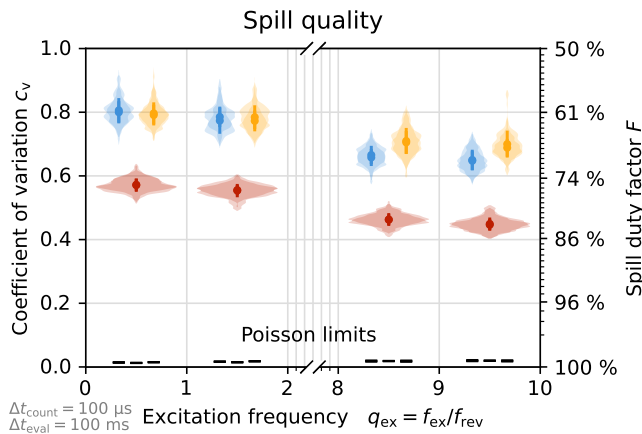
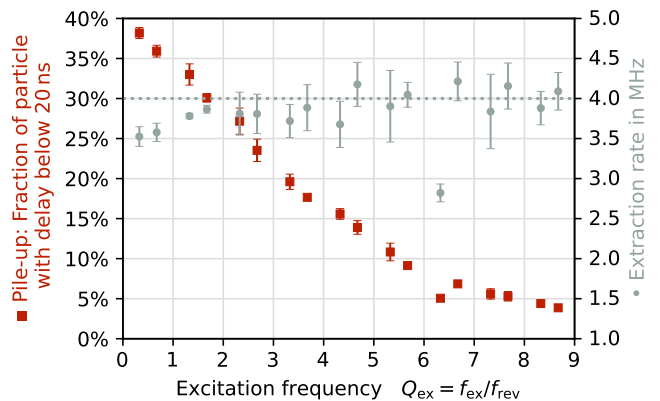


FIG. 14. Measurement of the spill quality for single-band noise excitation (blue and orange) and dual-band excitation (red) at sidebands of different harmonics. The dual-band cases are plotted at a frequency inbetween the two neighboring excitation bands they comprise.



been reported so far. The same applies to bunched beam extraction, where the frequency and harmonics of the bunching cavity are imprinted onto the spill [29–31]. The present study shows, that the undesired high frequency imprint can be mitigated when utilizing high frequency excitation at betatron sidebands of higher harmonics, due to the increased intrinsic width of these sidebands for particles near the separatrix. This has the benefit of a further spill quality improvement while allowing for an optimal choice of the excitation frequency to mitigate pile-up. In addition, simulations suggest that only a few dB of additional excitation power are required for the high frequency excitation, since the method does not rely on using narrowband or sinusoidal excitation, but instead uses efficient signals such as band-filtered noise covering the full sideband width.

VII. ACKNOWLEDGEMENTS

We thank Christian Schömers and Marcel Hun for support in preparing and conducting the measurement at HIT. We thank C. Cortés for valuable discussions on his studies at HIT and related simulations.

-
- [1] K. Hiramoto and M. Nishi, Resonant beam extraction scheme with constant separatrix, *Nucl. Instrum. Methods Phys. Res., Sect. A* **322**, 154 (1992).
 - [2] M. Tomizawa, M. Yoshizawa, K. Chida, J. Yoshizawa, Y. Arakaki, R. Nagai, A. Mizobuchi, A. Noda, K. Noda, M. Kanazawa, A. Ando, H. Muto, and T. Hattori, Slow beam extraction at TARN II, *Nucl. Instrum. Methods Phys. Res., Sect. A* **326**, 399 (1993).
 - [3] M. Benedikt, P. J. Bryant, L. Badano, M. Crescenti, P. Holy, A. T. Maier, M. Pullia, S. Rossi, and P. Knaus, *Proton-Ion Medical Machine Study (PIMMS): Part I*, Tech. Rep. CERN/PS 99-010 (DI) (Geneva, 1999).
 - [4] C. Belver-Aguilar, A. Faus-Golfe, F. Toral, and M. J. Barnes, Stripline design for the extraction kicker of compact linear collider damping rings, *Phys. Rev. ST Accel. Beams* **17**, 071003 (2014).
 - [5] M.-R. Mohammadian-Behbahani and S. Saramad, A comparison study of the pile-up correction algorithms, *Nucl. Instrum. Methods Phys. Res., Sect. A* **951**, 163013 (2020).
 - [6] R. Singh, P. Forck, P. Boutachkov, S. Sorge, and H. Welker, Slow extraction spill characterization from micro to milli-second scale, *J. Phys. Conf. Ser.* **1067**, 072002 (2018).
 - [7] S. van der Meer, *Stochastic Extraction, a Low-Ripple Version of Resonant Extraction*, Tech. Rep. CERN-PS-AA-78-6 (CERN, 1978).
 - [8] R. Cappi and Ch. Steinbach, Low frequency duty factor improvement for the CERN PS slow extraction using rf phase displacement techniques, *IEEE Trans. Nucl. Sci.* **28**, 2806 (1981).

- [9] G. Molinari and H. Mulder, The improved ultra-slow extraction noise system at LEAR, in *Proc. 4th European Particle Accelerator Conf.*, European Particle Accelerator Conference (London, UK, 1994).
- [10] K. Noda, T. Furukawa, S. Shibuya, T. Uesugi, M. Muramatsu, M. Kanazawa, E. Takada, and S. Yamada, Advanced RF-KO slow-extraction method for the reduction of spill ripple, *Nucl. Instrum. Methods Phys. Res., Sect. A* **492**, 253 (2002).
- [11] K. Noda, T. Furukawa, S. Shibuya, M. Muramatsu, T. Uesugi, M. Kanazawa, M. Torikoshi, E. Takada, and S. Yamada, Source of spill ripple in the RF-KO slow-extraction method with FM and AM, *Nucl. Instrum. Methods Phys. Res., Sect. A* **492**, 241 (2002).
- [12] T. Furukawa and K. Noda, Contribution of synchrotron oscillation to spill ripple in rf-knockout slow-extraction, *Nucl. Instrum. Methods Phys. Res., Sect. A* **539**, 44 (2005).
- [13] T. Nakanishi and K. Tsuruha, Simulation study of beam extraction from a synchrotron using colored noise with digital filter, *Nucl. Instrum. Methods Phys. Res., Sect. A* **608**, 37 (2009).
- [14] T. Nakanishi, Dependence of a frequency bandwidth on a spill structure in the rf-knockout extraction, *Nucl. Instrum. Methods Phys. Res., Sect. A* **621**, 62 (2010).
- [15] K. Mizushima, T. Shirai, T. Furukawa, and K. Noda, Making beam spill less sensitive to power supply ripple in resonant slow extraction, *Nucl. Instrum. Methods Phys. Res., Sect. A* **638**, 19 (2011).
- [16] R. Singh, P. Forck, and S. Sorge, Reducing fluctuations in slow-extraction beam spill using transit-time-dependent tune modulation, *Phys. Rev. Appl.* **13**, 10.1103/PhysRevApplied.13.044076 (2020).
- [17] T. Yamaguchi, Y. Okugawa, T. Shiokawa, T. Kurita, and T. Nakanishi, Slow beam extraction from a synchrotron using a radio frequency knockout system with a broadband colored noise signal, *Nucl. Instrum. Methods Phys. Res., Sect. B* **462**, 177 (2020).
- [18] E. C. Cortés García, E. Feldmeier, M. Galonska, C. Schömers, M. Hun, S. Brons, R. Cee, S. Scheloske, A. Peters, and T. Haberer, Optimization of the spill quality for the hadron therapy at the heidelberg ion-beam therapy centre, *Nucl. Instrum. Methods Phys. Res., Sect. A* **1040**, 167137 (2022).
- [19] P. Niedermayer and R. Singh, Excitation of nonlinear second order betatron sidebands for knock-out slow extraction at the third-integer resonance, *Phys. Rev. Accel. Beams* **27**, 082801 (2024).
- [20] G. Iadarola, R. D. Maria, S. Łopaciuk, A. Abramov, X. Buffat, D. Demetriadou, L. Deniau, P. D. Hermes, P. Kicsiny, P. Kruyt, A. Latina, L. Mether, K. Paraschou, G. Sterbini, F. F. Van der Veken, P. Belanger, P. Niedermayer, D. Di Croce, T. Pieloni, L. van Riesen-Haupt, and M. Seidel, Xsuite: An integrated beam physics simulation framework, in *Proc. 68th Adv. Beam Dyn. Workshop High-Intensity High-Brightness Hadron Beams*, Advanced Beam Dynamics Workshop on High-Intensity and High-Brightness Hadron Beams (JACoW Publishing, Geneva, Switzerland, 2023) pp. 73–80.
- [21] C. Kleffner, D. Ondreka, U. Weinrich, F. D. McDaniel, and B. L. Doyle, The Heidelberg ion therapy (HIT) accelerator coming into operation, in *AIP Conf. Proc.*, AIP Conference Proceedings, Vol. 1099 (AIP Conference Proceedings, Fort Worth, TX, USA, 2009) pp. 426–428.
- [22] S. White, E. Maclean, and R. Tomás, Direct amplitude detuning measurement with ac dipole, *Phys. Rev. ST Accel. Beams* **16**, 10.1103/PhysRevSTAB.16.071002 (2013).
- [23] P. Niedermayer and R. Singh, Excitation signal optimization for minimizing fluctuations in knock out slow extraction, *Sci Rep* **14**, 10310 (2024).
- [24] R. Singh, P. Boutachkov, P. Forck, P. Kowina, P. Schmid, A. Stafiniak, and H. Welker, Study of SIS-18 spill structure by introducing external ripples, in *GSI Scientific Report 2016*, GSI Report, edited by K. Große (GSI, Darmstadt, 2017) p. 447.
- [25] D. Boussard, Schottky noise and beam transfer function diagnostics, in *Proc. CERN Accelerator School: Advanced Accelerator Physics Course*, CAS - CERN Accelerator School (CERN, Rhodes, Greece, 1993, 1995) pp. 749–782.
- [26] E. C. Cortés García, P. Niedermayer, R. Singh, R. Taylor, E. Benedetto, E. Feldmeier, M. Hun, and T. Haberer, Interpretation of the horizontal beam response near the third integer resonance, *Phys. Rev. Accel. Beams* **27**, 124001 (2024).
- [27] P. Niedermayer, R. Singh, and R. Geißler, Software-defined radio based feedback system for beam spill control in particle accelerators, in *Proc. 13th GNU Radio Conf.*, GNU Radio Conference (GNU Radio Journal, Tempe, AZ, USA, 2023).
- [28] P. Virtanen, R. Gommers, T. E. Oliphant, M. Haberland, T. Reddy, D. Cournapeau, E. Burovski, P. Peterson, W. Weckesser, J. Bright, S. J. van der Walt, M. Brett, J. Wilson, K. J. Millman, N. Mayorov, A. R. J. Nelson, E. Jones, R. Kern, E. Larson, C. J. Carey, Í. Polat, Y. Feng, E. W. Moore, J. VanderPlas, D. Laxalde, J. Perktold, R. Cimrman, I. Henriksen, E. A. Quintero, C. R. Harris, A. M. Archibald, A. H. Ribeiro, F. Pedregosa, P. van Mulbregt, SciPy 1.0 Contributors, A. Vijaykumar, A. P. Bardelli, A. Rothberg, A. Hilboll, A. Kloeckner, A. Scopatz, A. Lee, A. Rokem, C. N. Woods, C. Fulton, C. Masson, C. Häggström, C. Fitzgerald, D. A. Nicholson, D. R. Hagen, D. V. Pasechnik, E. Olivetti, E. Martin, E. Wieser, F. Silva, F. Lenders, F. Wilhelm, G. Young, G. A. Price, G.-L. Ingold, G. E. Allen, G. R. Lee, H. Audren, I. Probst, J. P. Dietrich, J. Silterra, J. T. Webber, J. Slavič, J. Nothman, J. Buchner, J. Kulick, J. L. Schönberger, J. V. de Miranda Cardoso, J. Reimer, J. Harrington, J. L. C. Rodríguez, J. Nunez-Iglesias, J. Kuczynski, K. Tritz, M. Thoma, M. Newville, M. Kümmerer, M. Bolingbroke, M. Tartre, M. Pak, N. J. Smith, N. Nowaczyk, N. Shebanov, O. Pavlyk, P. A. Brodtkorb, P. Lee, R. T. McGibbon, R. Feldbauer, S. Lewis, S. Tygier, S. Sievert, S. Vigna, S. Peterson, S. More, T. Pudlik, T. Oshima, T. J. Pingel, T. P. Robitaille, T. Spura, T. R. Jones, T. Cera, T. Leslie, T. Zito, T. Krauss, U. Upadhyay, Y. O. Halchenko, and Y. Vázquez-Baeza, Scipy 1.0: Fundamental algorithms for scientific computing in python, *Nat. Methods* **17**, 261 (2020).
- [29] K. Gross, B. Zipfel, D. Lens, H. Klingbeil, J. Schmidt, P. Hülsmann, P. Spiller, R. Balss, T. Winnefeld, and U. Laier, Development of a spill-structure manipulation cavity and first experiment with beam in SIS18, in *Proc. 15th Int. Particle Accelerator Conf.*, International Particle Accelerator Conference (JACoW Publishing, Nashville, TN, USA, 2024) pp. 1432–1435.

- [30] S. Sorge, P. Forck, and R. Singh, Spill ripple mitigation by bunched beam extraction with high frequency synchrotron motion, *Phys. Rev. Accel. Beams* **26**, 014402 (2023).
- [31] J. Yang, Nano-second time scale measurements of the particle arrival times (Slow Extraction Workshop, MedAustron, Wiener Neustadt, 2024).